

# The Saturation of the Infrared Absorption by Carbon Dioxide in the Atmosphere

Dieter Schildknecht

Fakultät für Physik, Universität Bielefeld  
D-33501 Bielefeld, Germany

## Abstract

Based on new radiative transfer numerical evaluations, we reconsider an argument presented by Schack in 1972 that says that saturation of the absorption of infrared radiation by carbon dioxide in the atmosphere sets in as soon as the relative concentration of carbon dioxide exceeds a lower limit of approximately 300 ppm. We provide a concise brief and explicit representation of the greenhouse effect of the earth's atmosphere. We find an equilibrium climate sensitivity (temperature increase  $\Delta T$  due to doubling of atmospheric  $CO_2$  concentration) of  $\Delta T \simeq 0.5^0C$ .

# 1 Introduction.

In view of the immense literature concerning the effect of an (anthropogenic) increase in the relative atmospheric carbon dioxide concentration on the earth's climate, it is appropriate to revive a simple argument on this subject presented by Schack [1] in 1972. The three-page article published in German in the journal of the German Physical Society, at that time called "Physikalische Blätter", appeared under the title "Der Einfluß des Kohlendioxid-Gehalts der Luft auf das Klima der Welt", i.e. "The influence of the carbon dioxide content of the air on the climate of the world". The author, Schack, an expert on heat transfer in combustion devices, in 1923 had discovered the role played by the interaction of infrared electromagnetic radiation with carbon dioxide,  $CO_2$ , and water vapor,  $H_2O$ , in such devices [2].

The intensity of (monochromatic) radiation transversing an absorbing medium decreases exponentially with distance according to what is known as Lambert-Beer's law,

$$I(z) = I(z = 0)e^{-\kappa z}. \quad (1.1)$$

Independently of the numerical value of the absorption constant  $\kappa$  in (1.1), for sufficiently large distance,  $z$ , the limit of "complete absorption", or zero intensity of the outgoing radiation,  $I(z \rightarrow \infty) \rightarrow 0$ , is reached. For finite values of the exponent  $-\kappa z$  in (1.1), the numerical value of the  $\kappa$  determines the distance,  $z_\epsilon(\kappa)$ , for "approximate saturation",  $\exp(-\kappa z_\epsilon(\kappa)) = \epsilon \ll 1$ , or equivalently, "almost full absorption",

$$\frac{I(z = 0) - I(z = z_\epsilon(\kappa))}{I(z = 0)} = 1 - \frac{I(z = z_\epsilon(\kappa))}{I(z = 0)} = 1 - \epsilon. \quad (1.2)$$

In the case of  $CO_2$  in air, the wide band absorption constant  $\kappa$  for the infrared electromagnetic radiation depends on the concentration, or the partial pressure, of the  $CO_2$ , and a natural question concerns the magnitude of the  $CO_2$  concentration that leads to approximate saturation within the troposphere of the earth.

In his 1972 article [1], Schack points out that for a concentration of 0.03 % carbon dioxide in air, approximate saturation is reached within a distance of approximately the magnitude of the height of the troposphere. The absorption reaches values close to 100 % for a realistic  $CO_2$  content of 0.03 %, it is concluded [1] that any further increase of (anthropogenic)  $CO_2$  cannot lead to an appreciably stronger absorption of radiation, and consequently cannot affect the earth's climate.

It will be useful to elaborate on the argument given by Schack in detail, in order to explicitly display the simplicity and generality of the underlying concepts that lead to a parameter-free prediction of the absorption of infrared radiation by  $CO_2$ .

Adopting Planck's radiation law for a temperature at the surface of the earth, chosen as  $T = 293K$  by Schack, and taking into account the well-known absorption spectrum of the  $CO_2$  molecule, one finds that the radiation of wave lengths  $\lambda_{CO_2}$  in the interval  $13 \mu m \leq \lambda_{CO_2} \leq 17.6 \mu m$  is relevant for the absorption by  $CO_2$ . The total absorption due to  $CO_2$  in the atmosphere is determined by the total mass of  $CO_2$  that is transversed

by a beam of infrared radiation on its path from the surface at  $z = 0$  to the upper end of the atmosphere, or  $z \rightarrow \infty$ .

In the gravitational field of the earth, the pressure,  $p$ , of a gas decreases with increasing altitude,  $z$ , according to  $dp = -\rho g dz$ , where  $\rho$  denotes the density of the gas and  $g$  the acceleration due to gravity. For an ideal gas of temperature  $T$ , we have  $p = \rho RT/M$ , or  $\rho = pM/RT$ , with  $R$  being the gas constant,  $T$  denoting the absolute temperature and  $M$  the molecular weight of the gas. The total mass per unit area transversed by a beam of infrared radiation on its path through the atmosphere is determined by an integration over the density  $\rho(p, T)$  from the surface to the upper end of the troposphere. The result of the integration may be represented in terms of an effective altitude  $z_0$  of a fictitious atmosphere of homogeneous constant pressure  $p_0$ , constant temperature  $T$  and constant density  $\rho$ . The value of  $z_0$  (obviously) depends on whether the atmosphere is treated isothermally, or rather more realistically, is described adiabatically.

Adopting  $T = \text{const}$ , the decrease of pressure with increasing altitude becomes equal to

$$p(z) = p_0 \exp\left(-\frac{Mg}{RT}z\right), \quad (1.3)$$

which is the well-known barometric formula. The density  $\rho = \rho(z)$  decreases accordingly as

$$\rho(z) = \frac{M}{RT}p_0 \exp\left(-\frac{z}{z_0}\right) \equiv \rho_0 \exp\left(-\frac{z}{z_0}\right), \quad (1.4)$$

where

$$z_0 = \frac{RT}{Mg} \quad (1.5)$$

denotes the scale-height of the atmosphere, the height of a fictitious atmosphere of homogeneous pressure  $p_0$ , temperature  $T$  and density  $\rho_0$ , and a mass per unit area,  $M_0$ , obtained from (1.4),

$$M_0 \equiv \int_0^\infty \rho(z) dz = \rho_0 z_0 = \frac{M p_0}{R T} z_0. \quad (1.6)$$

The determination of the absorption of the atmosphere is accordingly reduced to the evaluation of the absorption by a gas pipe of length  $z_0$  from (1.5) homogeneously filled with air, and with  $CO_2$  of partial pressure  $p_0 \equiv p_{CO_2}$ , at a total pressure of 1 atm at temperature  $T = 293 K$ .

For the realistic case of an adiabatically treated atmosphere relation (1.6) remains valid with an appropriately chosen value of  $z_0$  different from (1.5). In our approach of Section 2 the value of  $z_0$  will be determined from the altitude dependence of the absorption of infrared radiation for given lapse rate in the atmosphere.

The absorption due to (1.1), upon introducing the dependence on the  $CO_2$  concentration via the partial pressure  $p_{CO_2}$ , becomes

$$A(p_{CO_2}, z_0) = 1 - \exp(-ap_{CO_2}z_0), \quad (1.7)$$

where the coefficient  $a$  must be determined from the known absorption spectrum of  $CO_2$ . Since the absorption cross section of  $CO_2$  depends on the wave length of the radiation

being absorbed, the absorption constant  $a$  in (1.7), obtained by summation over a spectrum of a large number of spectral lines, actually develops a dependence on the partial pressure  $p_{CO_2}$ .

$CO_2$ [%]	0.03 %	0.06 %	$\Delta_{2 \times CO_2}$ [%]	$\Delta_{2 \times CO_2}$ [ $Wm^{-2}$ ]
$p_{CO_2} z_0$ [ $atm \times m$ ]	2.1	4.2		
A [%]	98.5 %	99.3 %	0.8 %	0.70
1 - A [%]	1.5 %	0.7 %		
$a$ [ $(atm \times m)^{-1}$ ]	2.0	1.73		

Table 1: The results given in the first four horizontal lines are taken from ref. [1], the results in the last line are computed using (1.7).

In his article [1], addressing the question on the effect of an increase of the  $CO_2$  concentration on the climate on earth, Schack compares the absorption due to  $CO_2$ , by a  $CO_2$ -air pipe as mentioned, for a partial pressure corresponding to a realistic value of 300 ppm = 0.03 % with the absorption due to an enhanced value taken as 600 ppm = 0.06 %<sup>1</sup>, respectively corresponding to  $p_{CO_2} = 3 \times 10^{-4}$  atm and  $p_{CO_2} = 6 \times 10^{-4}$  atm at  $T = 293$  K and a total pressure of 1 atm of the atmosphere. Adopting  $z_0 = 7000$  m for the equivalent height of the troposphere, for the absorption, A [%], and the increase of absorption,  $\Delta_{2 \times CO_2}$ , Schack obtains the results that are given in Table 1.

Saturation of infrared radiation by the realistic  $CO_2$  content of the atmosphere of 0.03 % being reached within approximately 1 % according to Table 1, any further increase of the  $CO_2$  content does not substantially increase the absorption of radiation, and accordingly does not affect [1] the climate on earth.

The results on  $\Delta_{2 \times CO_2}$  [%] in Table 1 refer to the radiation in the  $CO_2$  band of  $13 \mu m \lesssim \lambda_{CO_2} \lesssim 17.6 \mu m$  ( $568 cm^{-1} \lesssim 1/\lambda_{CO_2} \lesssim 769 cm^{-1}$ ). With the assumption of a black-body radiation at  $T = 293 K$ , the input radiation in the  $CO_2$  band amounts to  $87 W/m^2$ . The additional absorption due to  $CO_2$  doubling is given by  $\Delta_{2 \times CO_2} \times 87 W/m^2 = 0.8 \times 10^{-2} \times 87 W/m^2 = 0.70 W/m^2$ , as listed in Table 1. This increase of the absorption of infrared radiation in the atmosphere is indeed negligible in comparison with the equilibrium value of the total outgoing long-wave infrared radiation (LWIR) at the top of the atmosphere (TOA) given by  $S_0 = 239 W/m^2$ .<sup>2</sup>

<sup>1</sup> A realistic value for the increase of the  $CO_2$  concentration per year is 2 ppm/year, e.g. [3], implying 150 years for the doubling of a  $CO_2$  concentration of 300 ppm.

<sup>2</sup>The known empirical value of the sun radiation of  $1365 W/m^2$  with an albedo of 0.3 yields  $956 W/m^2$  absorption. Dividing by 4 to take into account the surface of the earth yields the average value of the radiation from the sun to be balanced by the outgoing average LWIR of  $S_0 = 239 W/m^2$  [4].

## 2 Absorption of Infrared Radiation: $CO_2$ -Air Pipe versus Atmosphere.

Using presently available detailed data on the spectral absorption lines of  $CO_2$ , compare [5], the absorption coefficient<sup>3</sup>  $a$  and the resulting absorption by a  $CO_2$ -air pipe, defined before, can be reliably predicted. In this Section, we compare the results on absorption by a  $CO_2$ -air pipe at fixed temperature and pressure, as a function of the length of the  $CO_2$ -air pipe, with the absorption by an adiabatically treated atmosphere. The results to be presented are due to a recent evaluation by Clark [7] for the  $^{12}C\ ^{16}O_2$  molecule only, with linestrengths  $> 10^{-23}$ . We refer to Appendix A for further details.

	A 300 ppm	A 600 ppm	$\Delta_{2\times CO_2}$ [ % ]	$\Delta_{2\times CO_2}$ [ $Wm^{-2}$ ]
1 km	0.63	0.71	8 %	7.00
2 km	0.71	0.78	7 %	6.09
3 km	0.75	0.82	7 %	6.09
5 km	0.81	0.87	6 %	5.22
7 km	0.84	0.89	5 %	4.35

Table 2a:  $CO_2$ -air pipe absorption A and increase  $\Delta_{2\times CO_2}$  for selected path lengths and  $CO_2$  concentrations for the spectral range  $568$  to  $769$   $cm^{-1}$  (input black-body radiation  $87$   $Wm^{-2}$ ) and  $T = 293K$ ,  $p = 1atm$ . Compare Appendix A Table A2.

	A 300 ppm	A 600 ppm	$\Delta_{2\times CO_2}$ [ % ]	$\Delta_{2\times CO_2}$ [ $Wm^{-2}$ ]
1 km	0.79	0.87	8 %	5.20
2 km	0.87	0.93	6 %	3.90
3 km	0.91	0.96	5 %	3.25
5 km	0.95	0.98	3 %	1.95
7 km	0.97	0.99	2 %	1.30

Table 2b: Same as Table 2a, but for  $600$   $cm^{-1}$  to  $750$   $cm^{-1}$  spectral range (input black-body radiation  $65$   $Wm^{-2}$ ). Compare Appendix A Table A3.

The results [7] for the absorption of a  $CO_2$ -air pipe for the spectral range of  $13\mu m \lesssim \lambda_{CO_2} \lesssim 17.6\mu m$  ( $568$   $cm^{-1}$  to  $769$   $cm^{-1}$ ), as a function of selected values of the path length (pipe length) and the relevant  $CO_2$  concentrations of 0.03 % and 0.06 % are shown in Table

<sup>3</sup>Compare e.g. ref. [6] for a recent evaluation of absorption coefficients

2a. The pipe is assumed to have constant temperature,  $T = 293\text{ K}$ , and a total pressure of  $p = 1\text{ atm}$ . The input black-body infrared radiation at  $T = 293\text{ K}$  is accordingly given by  $87\text{ W m}^{-2}$ . The results in Table 2a explicitly demonstrate the expected increase of the absorption  $A$  with increasing length of the pipe (path length), as well as the decrease of the relative absorption for  $\text{CO}_2$  doubling,  $\Delta_{2\times\text{CO}_2} [\%]$ . The result of  $\Delta_{2\times\text{CO}_2} = 5\%$  at the pipe length of 7 km is considerably larger than the 1972 result of  $\Delta_{2\times\text{CO}_2} = 0.8\%$  given in Table 1.

In table 2b, for illustration, we show the effect of restricting the spectral range of the input black-body radiation to the spectral range of  $600\text{ cm}^{-1}$  to  $750\text{ cm}^{-1}$  (total black-body radiation  $65\text{ W m}^{-2}$ ). Comparing the results in Table 2b with the ones in Table 2a, we notice the more rapid approach to a (larger) asymptotic absorption limit with increasing path length of the infrared radiation. This is a consequence of the change of absorbance as a function of the spectral wave length taken into account.

In fig. 1, we show the calculated spectrum of the absorbance for the case of a path length of 3 km and a  $\text{CO}_2$  concentration of 0.03% and 0.06%. The spectral ranges corresponding to Tables 2a and 2b are indicated in fig. 1.

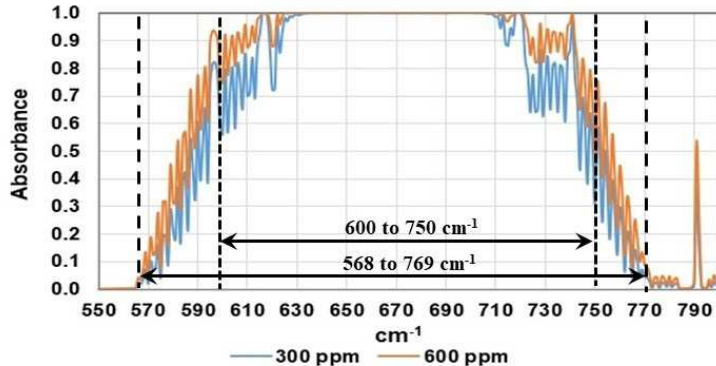


Figure 1: The absorbance of 0.03 % and 0.06 % concentrations of  $\text{CO}_2$  in dry air at 293 K for a 3 km  $\text{CO}_2$ -air pipe. The spectral ranges of  $568$  to  $769\text{ cm}^{-1}$  and  $600$  to  $750\text{ cm}^{-1}$  used in the absorption band calculations are indicated. The calculation [7] was performed at a spectral resolution of  $0.01\text{ cm}^{-1}$ , but the data are plotted at  $1\text{ cm}^{-1}$ .

Turning from fixed temperature  $T$  in the  $\text{CO}_2$ -air pipe to decreasing  $T$  and pressure  $p$  in the atmosphere, we proceed in two steps. In a first step, modelling a dry atmosphere, we consider the effect of  $\text{CO}_2$  (at concentrations of 0.03% and 0.06%), and in a second step, we add water vapor of fixed relative humidity (RH) chosen as  $\text{RH} = 85\%$ .

In table 3a, we show the results for the absorption  $A$  of the atmosphere at several selected altitudes for a  $\text{CO}_2$  content of 0.03% and 0.06%. The spectral range of the LWIR of  $568\text{ cm}^{-1}$  to  $769\text{ cm}^{-1}$  is identical to the spectral range employed for the results in Table 2a. The evaluation of the absorption was carried out for a surface temperature of  $T = 293\text{ K}$  and a surface pressure  $p = 1\text{ atm}$ , and a realistic moist adiabatic lapse rate increasing with altitude, and an average value of  $-6.5\text{ }^{\circ}\text{C km}^{-1}$  was employed (compare

	A 300 ppm	A 600 ppm	$\Delta_{2\times CO_2}$ [ % ]	$\Delta_{2\times CO_2}$ [ $Wm^{-2}$ ]
Atm 5 km	0.74	0.81	7 %	6.09
Atm 9 km	0.76	0.83	7 %	6.09
Atm 11 km	0.76	0.83	7 %	6.09

Table 3a: Altitude dependence of the infrared absorption  $A$  by the atmosphere for selected altitudes and  $CO_2$  concentrations for the  $568$  to  $769$   $cm^{-1}$  spectral range (input black-body radiation  $87$   $Wm^{-2}$ ). Surface temperature and surface pressure are  $T = 293$  K and  $p = 1$  atm, and the lapse rate adopted for the atmosphere is given by  $-6.5$   $^0Ckm^{-1}$ . Compare Appendix A Table A4.

	A 300 ppm	A 600 ppm	$\Delta_{2\times CO_2}$ [ % ]	$\Delta_{2\times CO_2}$ [ $Wm^{-2}$ ]
Atm 5 km	0.90	0.95	5 %	3.25
Atm 9 km	0.91	0.96	5 %	3.25
Atm 11 km	0.91	0.96	5 %	3.25

Table 3b: Same as Table 3a, but for a  $600$  to  $750$   $cm^{-1}$  spectral range (input black body emission  $65$   $Wm^{-2}$ ). Compare Appendix A Table A4.

Appendix A, fig. A6). The absorption spectrum at  $0.01$   $cm^{-1}$  resolution was calculated using a spatial resolution of 100 m. The absorption spectrum for each 100 m level was calculated using the pressure and temperature for that level derived from the lapse rate. The results in Table 3a show a rapid convergence to an approximately constant, quasi-asymptotic behavior of the absorption  $A$  that is reached above an altitude of approximately 5 km. By comparison of the results in Table 3a with the ones in Table 2a, we conclude that a  $CO_2$ -air pipe for a chosen length of 2 to 3 km represents the absorption of the atmosphere that reaches a quasi-asymptotic limit at altitudes of about 5 km. The values of the absorption and the increase of the absorption under  $CO_2$  doubling of  $\Delta_{2\times CO_2} = 7\%$  corresponding to  $6Wm^{-2}$  in Tables 2a and 3a are in agreement with each other. Similar conclusions are drawn from the comparison of the results for the restricted spectral range in Tables 2b and 3b with each other.

In fig. 2, we show the absorption of the surface emission at 293 K of 300 and 600 ppm of  $CO_2$  for the dry atmosphere looking downwards from a height of 7 km. The total spectral range is from  $550$  to  $800$   $cm^{-1}$  and the spectral intervals are indicated. These are the same as for fig. 1. The spectral resolution of the calculation was  $0.01$   $cm^{-1}$  with a spatial resolution of 100 m. The spectral resolution of the plot however, is  $1$   $cm^{-1}$ . This spectrum includes the effects of the decrease in temperature and pressure with altitude as shown in Appendix A, fig. A6. In this case most of the absorption occurs near the

surface and the value of the total absorption tends towards an asymptotic value as the altitude increases. This is shown in Appendix A, fig. A4.

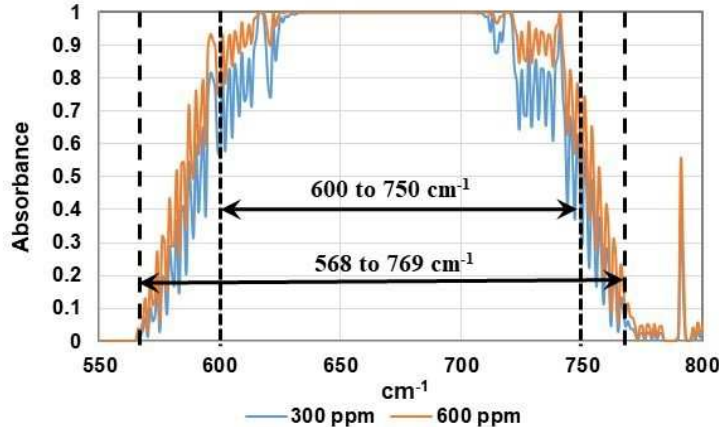


Figure 2: The absorbance of 0.03 % and 0.06 % concentrations of  $CO_2$  in a dry atmosphere for a vertical path length from the surface to 7 km altitude. The surface temperature is 293 K. The lapse rate is  $-6.5 \text{ K km}^{-1}$  and the spatial resolution is 100 m. The calculation [7] was performed at a spectral resolution of  $0.01 \text{ cm}^{-1}$ , but the data are plotted at  $1 \text{ cm}^{-1}$  resolution.

The results explicitly demonstrate that the  $CO_2$ -air pipe of path length of approximately 3 km represents the absorption in the atmosphere of a quasi-asymptotic altitude reached at 5 km.

	A 300 ppm	A 600 ppm	$\Delta_{2\times CO_2}$ [ % ]	$\Delta_{2\times CO_2}$ [ $Wm^{-2}$ ]
Atm 5 km 85 RH	0.89	0.92	3 %	2.6
Atm 9 km 85 RH	0.90	0.93	3 %	2.6
Atm 11 km 85 RH	0.90	0.93	3 %	2.6

Table 4a: Same as Table 3a, but including the absorption by water vapor of relative humidity (RH) of 85 %. Compare Appendix A, Table A5.

The important role of water vapor – semi-quantitatively discussed in ref. [1] – is illustrated by comparing the results in Tables 3a and 3b with the results presented in Tables 4a and 4b. The results in Tables 4a and 4b, in addition to  $CO_2$ , take into account water vapor with relative humidity (RH) of  $RH = 85\%$ . The presence of water vapor

	A 300 ppm	A 600 ppm	$\Delta_{2\times CO_2}$ [ % ]	$\Delta_{2\times CO_2}$ [ $W m^{-2}$ ]
Atm 5 km 85 RH	0.94	0.97	3 %	2.0
Atm 9 km 85 RH	0.95	0.98	3 %	2.0
Atm 11 km 85 RH	0.95	0.98	3 %	2.0

Table 4b: Same as Table 3b, but including the absorption by water vapor of relative humidity (RH) of 85 %. Compare Appendix A, Table A5.

drastically reduces<sup>4</sup> the effect of doubling the  $CO_2$  concentration from  $6.09 W m^{-2}$  to about  $2.6 W m^{-2}$  for the infrared spectral range of  $568$  to  $769 cm^{-1}$ . A similar effect is seen by comparing the results in Tables 3b and 4b with each other.

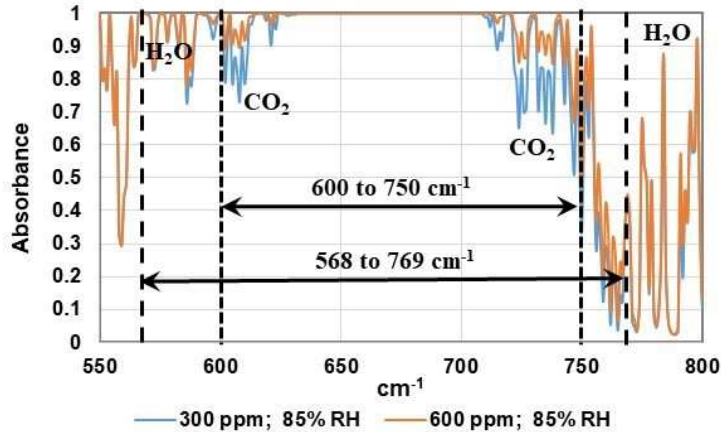


Figure 3: The absorbance of 0.03 % and 0.06 % concentrations of  $CO_2$  in a moist atmosphere for a vertical path length from the surface to 7 km altitude. The surface temperature is 293 K. The relative humidity at the surface is 85 %. The lapse rate is  $-6.5 K km^{-1}$  up to the saturation level the spatial resolution is 100 m. The calculation [7] was performed at a spectral resolution of  $0.01 cm^{-1}$ , but the data are plotted at  $1 cm^{-1}$  resolution.

For comparison with fig. 2, in fig. 3, we show the absorption spectrum in the atmosphere for the presence of water vapor in addition to carbon dioxide.

<sup>4</sup>Note that (obviously) the presence of water vapor increases the absorption of radiation. The presence of water vapor, however, decreases the effect of an increase of the  $CO_2$  concentration. Compare ref. [1] for a semi-quantitative discussion.

In summarizing this Section we conclude that a  $CO_2$ -air pipe of path length of 2 to 3 km represents the effect of the  $CO_2$  increase in the atmosphere which has reached its quasi-asymptotic saturation limit at an altitude of approximately 5 km. Inclusion of water vapor drastically reduces the effect on the absorption of a rise of the  $CO_2$  concentration from 0.03% to 0.06% from about  $6W\ m^{-2}$  to  $3W\ m^{-2}$ . The value of  $3W\ m^{-2}$  additional absorption corresponding to  $3/418 \simeq 0.7\%$  of the total outgoing radiation at the surface of the earth, we conclude that the doubling of the  $CO_2$  concentration for the relevant time scale of about a century is a fairly negligible one. Even though the increase of absorption of  $\Delta_{2\times CO_2} \simeq 3W\ m^{-2}$  is considerably larger than the 1972 value of  $\Delta_{2\times CO_2} \simeq 1W\ m^{-2}$ , the main conclusion from ref. [1] remains valid.

### 3 $CO_2$ Doubling and Surface Temperature

In Section 2, we concluded that the absorption of infrared radiation from the  $CO_2$  band in the atmosphere becomes (approximately) independent of the altitude for altitudes larger than about 5 km; the absorption reaches a quasi-asymptotic saturation limit at an altitude of about 5 km. The magnitude of the quasi-asymptotic absorption agrees with the absorption of a  $CO_2$ -air pipe at constant temperature,  $T = 293K$ , and constant pressure,  $p = 1atm$ , and length of about 2 to 3 km.

The evaluation [7], compare Appendix A for details, of the absorption by the atmosphere is based on the known spectroscopic properties of the absorbing gases,  $H_2O$ ,  $CO_2$ , and the empirically known average lapse rate of the atmosphere of about  $-6.5K\ km^{-1}$ . The absorption reaches an approximately constant value at an altitude of 6 km. At and beyond that height, a constant value of infrared radiation is freely emitted to space. At this height, the atmosphere provides a “free window” (compare Appendix B) for the emittance of infrared radiation at temperature  $T_{TOA} = (293 - 6 \times 6.5)K = 254K \simeq 255K$ . The outgoing intensity is given by  $S_{space} = S(T)|_{T=255K} = \sigma T^4|_{T=255} = 240\ W\ m^{-2}$ .

The approximate stability of the climate on earth, a necessary condition for life on earth, requires equilibrium of the outgoing infrared radiation, predicted by  $S_{space} = S(T)|_{T=255K}$ , with the effective radiation provided by the sun. The effective radiation by the sun amounts<sup>5</sup> to  $S_0 = 240W\ m^{-2}$ . The agreement of the above parameter-free prediction of the radiative transfer calculation, with the effective radiation from the sun,

$$S_{space} = S(T)|_{T=255K} = S_0, \quad (3.1)$$

provides a non-trivial support of the radiative-transfer calculation based on the empirical lapse rate of  $6.5K\ m^{-2}$ . Indeed, the radiative-transfer analysis explains the approximate stability of the climate on earth.

For a concise representation of the radiative “greenhouse effect” in terms of the radiation from the sun,  $S_0$ , and the earth’s LWIR within as well as outside the “atmospheric window”, as quantified by  $S_W$ , and the fractional transmittance,  $f' \ll 1$ , respectively, compare Appendix B.

---

<sup>5</sup>Compare footnote 3

	$\Delta_{2\times CO_2} [Wm^{-2}]$	$\Delta T [K]$
3 km $CO_2$ -air pipe 9 km Atmosphere	6.09	1.07
9 km Atmosphere $RH = 85\%$	2.6	0.46

Table 5: The increase of surface temperature compensating infrared absorption by  $CO_2$  and by  $CO_2 + H_2O$  with  $RH = 85\%$

We turn to the effect of  $CO_2$  doubling on the surface temperature. We assume the existence of radiative equilibrium of the emitted black-body LWIR, given by  $S(T)$ , for any given  $CO_2$  content (within the presently discussed limits). Absorption under doubling of the  $CO_2$  concentration,  $\Delta_{2\times CO_2}$ , for compensation requires increase of radiation  $S(T) \rightarrow S(T) + \Delta S$ , i.e.

$$S(T) + \Delta S = S(T + \Delta T) = S(T) + \left. \frac{dS}{dT} \right|_T \Delta T, \quad (3.2)$$

where  $\Delta S \equiv \Delta_{2\times CO_2}$  and  $T$  denotes the surface temperature, chosen as  $T = 293K$  in our treatment. Note that the detailed mechanism occurring in the atmosphere leading to the required increase of  $\Delta S = \Delta_{2\times CO_2}$  need not be specified. According to (3.2), the temperature has to rise by

$$\Delta T = \frac{\Delta_{2\times CO_2}}{\left( \frac{dS}{dT} \right)_T} = \frac{T \Delta_{2\times CO_2}}{4S(T)}, \quad (3.3)$$

where  $S(T) \sim T^4$  for a Planck radiator is used in the last step. Relation (3.3) specifies the rise of the surface temperature connected with restoration of equilibrium at the end of a  $CO_2$ -air pipe, or equivalently, at the altitude of the atmosphere where the quasi-asymptotic limit of the absorption has been reached. Inserting  $T = 293K$ , and  $S(T = 293K) = 418Wm^{-2}$ , as well as  $\Delta_{2\times CO_2} = 6.09W m^{-2}$  from Tables 2a and 3a into (3.3), we obtain an increase of surface temperature of  $\Delta T = 1.07 K$ , compare Table 5. Insertion of  $\Delta_{2\times CO_2} = 2.6W m^{-2}$  from Table 4a into (3.3) shows the strong effect of water vapor of  $RH = 85\%$ . The strong absorption due to  $H_2O$  diminishes the surface-temperature change to  $\Delta T = 0.46K$  for the assumed increase of the  $CO_2$  concentration from 0.03% to 0.06%.

## 4 Radiative Absorbance under Change of Atmospheric Conditions.

A very elaborate radiative transfer calculation, recently presented by Harde [10], within a two-layer climate model, explores<sup>6</sup> the infrared absorbance by  $CO_2$  under a variety of

---

<sup>6</sup>Compare refs. [8, 9] for alternative dynamical climate models.

atmospheric conditions, such as surface temperature, humidity, clouds etc. Results [10] on the radiative absorbance for  $CO_2$  contents of 380 ppm and 760 ppm, under variation of the atmospheric conditions, are shown in Table 6.

0.038 %	0.076 %	$\Delta_{2\times CO_2}$ [%]	$\Delta_{2\times CO_2}$ [ $Wm^{-2}$ ]	$\Delta T$ [K]	$\overline{\Delta}_{2\times CO_2}$ [ $Wm^{-2}$ ]	$\overline{\Delta T}$ [K]
82.57 %	83.84 %	1.27 %	5.03	0.92		
82.57 %	83.31 %	0.74 %	2.93	0.53	3.45	0.63
89.77 %	90.48 %	0.71 %	2.81	0.51		
81.55 %	82.05 %	0.50 %	1.98	0.36		
84.08 %	85.22 %	1.14 %	4.51	0.82		

Table 6: The first three columns quote the results obtained by Harde [10] for the absorbance of infrared radiation for  $CO_2$  concentrations of 0.038 % and 0.076 %, and the increase  $\Delta_{2\times CO_2}$  [%], under different atmospheric conditions, such as surface temperature, humidity, clouds etc. In the remaining four columns, we present the associated increase,  $\Delta_{2\times CO_2}$  [ $Wm^{-2}$ ], and the surface temperature increase,  $\Delta T$ , and the averages  $\overline{\Delta}_{2\times CO_2}$  and  $\overline{\Delta T}$ .

We note that the results for the absorbance in Table 6 give the absorption due to  $CO_2$  doubling as a fraction of the total LWIR of  $S(T) = 396 Wm^{-2}$  at  $T = 289 K$  employed by Harde, compared to Tables 2a,b through 4a,b that give the results for the increase of absorbance from  $CO_2$  doubling as a fraction of the radiation in the  $CO_2$  band. For a detailed discussion, we refer to ref. [10].

In the context of the present discussion, the essential and important point of the results in Table 6 is the approximate independence of the absorption due to  $CO_2$  doubling,  $\Delta_{2\times CO_2} \cong 1\%$ , from the various atmospheric conditions evaluated. Compare the results for  $\Delta_{2\times CO_2}$  in column 3 of Table 6. The spread of the results for  $\Delta T$  in column 5 of Table 6 between  $\Delta T = 0.36K$  and  $\Delta T = 0.92K$ , and the average value of  $\overline{\Delta T} = 0.63K$ , are consistent with the result from our straight-forward evaluation of  $\Delta T = 0.46K$  in Table 5.

The consistency or approximate agreement of our result of  $\Delta T = 0.46 \simeq 0.5K$  in Table 5, and the result of  $\overline{\Delta T} \cong 0.6K$  in Table 6 requires additional comments. The agreement strengthens the validity of our result based on what may be called a single-layer (surface) model, particularly evident from the equivalence of the atmosphere and the  $CO_2$ -air pipe running at surface temperature and surface pressure. On the other hand, we conclude that much of the involved details of various flux terms of a two-layer model can apparently be summarized by our simple radiative equilibrium assumption for  $\Delta T$  in (3.3). For a supplementary discussion on  $\Delta T$  we refer to the last part of Appendix B.

## 5 Conclusions

It has been the aim of this paper to estimate the increase in temperature  $\Delta T$  (“climate sensitivity”) of the surface of the earth due to a doubling of the  $CO_2$  concentration in the atmosphere. The estimate is obtained in a concise and transparent manner without oversimplification. All necessary steps are explicitly elaborated upon.

The basic assumption of associating a uniform constant temperature  $T$  with the surface of the earth, and a black-body long-wave infrared radiation  $S(T)$ , is by no means trivial, implicitly or explicitly, however, common to main-stream investigations on this matter. Our results are based on a new radiative-transfer evaluation, the details being presented in Appendix A. The absorption of the atmosphere in the  $CO_2$  spectral range can be, and is reliably determined, and leads to an approximately constant value beyond an altitude of about 5 km, or a length of the horizontal  $CO_2$ -air pipe of about 3 km at surface temperature and pressure.

Assuming restoration of equilibrium upon doubling of the  $CO_2$  concentration by an associated increase of the temperature then implies a definite estimate of the increase of the surface temperature  $\Delta T$ , given by  $\Delta T \cong 0.5^{\circ}C$  that confirms, or is being confirmed by, more detailed investigations in the literature.

The quantitative result of  $\Delta T \simeq 0.5$  to  $0.6^{\circ}C$  valid for the drastic increase of doubling of the  $CO_2$  content in air from 380 ppm to 760 ppm to be related to one century, confirms that the effect of an anthropogenic  $CO_2$  increase on the climate on earth is fairly negligible. This conclusion is in strong contrast to the values of  $\Delta T \sim 1.5 - 4.5^{\circ}C$  quoted in the 2013 IPCC report [11]. The published results<sup>7</sup> on  $\Delta T$  fill an even larger interval between  $\Delta T \simeq 0.4^{\circ}C$  to  $\Delta T \simeq 8^{\circ}C$ . There is a systematic tendency of the results on  $\Delta T$  published between the years 2000 to 2018 to decrease [12] with increasing publication date, the results coming closer to our result of  $\Delta T \simeq 0.5^{\circ}C$ . In this connection, compare also ref. [13] on “No Experimental Evidence for the Significant Anthropogenic Climate Change”.

We found a concise and brief derivation of the earth’s greenhouse effect (compare Appendix B, in particular figure B1). The greenhouse effect is explicitly derived. It is understood as a shift of the radiative equilibrium from the earth’s surface to an atmospheric level above approximately five kilometers.

## Acknowledgement

The author thanks Konrad Kleinknecht for discussions that initiated the present investigation. The author thanks Peng-Sheng Wei for a useful correspondence. Particular thanks go to Roy Clark for providing the radiative transfer results in Appendix A, for much help in tracing the relevant literature on the subject matter, as well as a critical reading of the present paper.

---

<sup>7</sup>Compare e.g. the list of references to published results on  $\Delta T$  in ref. [3]

## References

- [1] A. Schack, “Der Einfluß des Kohlendioxid-Gehaltes der Luft auf das Klima der Welt”, *Phys. Blätter* 28 (1972) 26-28.
- [2] A. Schack, *Der industrielle Wärmeübergang*, Verlag Stahleisen m.b.H. Düsseldorf, 1. Auflage 1929, 8. Auflage 1983.
- [3] F. Gervais, “Tiny warming of residual anthropogenic  $CO_2$ ”, *Internat. Journal of Mod. Phys. B* Vol. 28, No 13 (2014) 1450095, World Scientific;  
F. Gervais, *L'urgence climatique est un leurre*, 2018, Editions de l'Artilleur, 75008 Paris.
- [4] K.E. Trenberth, J.T. Fasullo and J. Kiehl, “Earth’s global energy budget”, *Bull. Am. Meteorol. Soc.* 90, 311 (2009).
- [5] HITRAN data base.
- [6] Peng-Shen Wei et al., “Absorption coefficient of carbon dioxide across atmospheric troposphere layer” *Heliyon* 2018; 4(10): e00785.
- [7] R. Clark, Ventura Photonics, private communication, see Appendix A.
- [8] R. Clark, “A dynamic coupled thermal reservoir approach to atmospheric energy transfer, part I: Concepts”, “A dynamic coupled thermal reservoir approach to atmospheric energy transfer, part II: Applications”, “A dynamic coupled thermal reservoir approach to atmospheric energy transfer, part V: Summary”, *Energy and Environment* 24 (3,4) 319 (2013), 24 (3,4) 341 (2013), Ventura Photonics Monograph VPM 005 (2019).
- [9] G.V. Chilinger et al., “Do increasing contents of methane and carbon dioxide in the atmosphere cause global warming?”, *Atmospheric and Climate Sciences*, 2014, 4, 819;  
O.G. Sorokhatin et al., *Global Warming and Global Cooling: Evolution of Climate on Earth*, Elsevier 2007.
- [10] H. Harde, “Radiation transfer calculations and assessment of global warming by  $CO_2$ ”, *Internat. Journal of Atmospheric Sciences*, Volume 2017, Article ID 9251034.
- [11] Fifth Assessment Report of the Intergovernmental Panel on Climate Change (IPCC), AR5, T.F. Stocker et al., Eds., *Climate Change 2013; The Physical Science Basis*, Cambridge University Press, New York, NY, USA, 2014.
- [12] F. Gervais, “Anthropogenic  $CO_2$  warming challenged by 60-year cycle”, *Earth Sciences Reviews* 155 (2016) 129.
- [13] J. Kauppinen and P. Malmi, “No experimental evidence for the significant anthropogenic climate change”, arXiv: 1907.00165v1 [physics.ao-ph].

- [14] A. A. Tsonis, *Atmospheric Thermodynamics*, 2nd Edition, Cambridge University Press, Cambridge UK, 2007.
- [15] Clark, R., “A dynamic coupled thermal reservoir approach to atmospheric energy transfer Part II: Applications” *Energy and Environment* 24(3, 4) 341-359 (2013).

# Appendices

## A $CO_2$ Absorbance 568 to 770 $cm^{-1}$ , 7 km path, 296 K, 300, 600 ppm

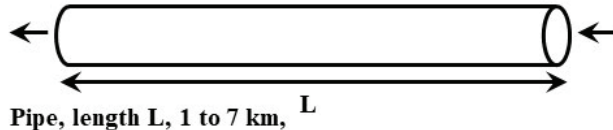
The configurations used for the pipe and atmospheric absorption calculations are shown in Figures A1a and A1b.

For the ‘pipe’ configuration, a variable horizontal path length  $L$ , from 1 to 7 km long was used. The  $CO_2$  concentration was varied from 280 to 1000 ppm. A total pressure of 1 atmosphere dry air at 293 K was used.

For the atmospheric absorption calculation, a vertical path,  $h$ , from 1 to 11 km was used. The surface temperature was set to 293 K at 1 atmosphere pressure. Two sets of calculations were performed. The first used dry air with a lapse rate of  $-6.5\text{ K km}^{-1}$ . The second used a surface relative humidity of 85 % with a lapse rate of  $-6.5\text{ K km}^{-1}$  up to the saturation level. Above the saturation level, the meteorological formula for the saturated lapse rate is used [14]. The lapse rates used are plotted below in Figure A6. The vertical atmospheric profile was calculated using a spatial resolution of 100 m.

The high resolution  $CO_2$  absorbance spectra were calculated using spectral data from the HITRAN database [5],  $^{12}C^{16}O_2$  lines only with linestrengths  $> 1e-23$ . The spectral resolution was  $0.01\text{ cm}^{-1}$ . The temperature was set to 293 K. For the ‘pipe’ calculations, the large spectral data files were divided into seven spectral ranges with the absorption coefficient calculated for each spectral range. The calculations were performed using Excel workbooks with each spectral range in a separate workbook. The weighted averages over the spectral ranges 568 to  $770\text{ cm}^{-1}$  and 600 to  $750\text{ cm}^{-1}$  were then calculated. The ‘pipe’ calculation is illustrated in Table A1. Path lengths of 1, 2, 3, 5 and 7 km were used. The results are given in Tables A2 and A3. Plots of the data are shown in Figures A2 and A3.

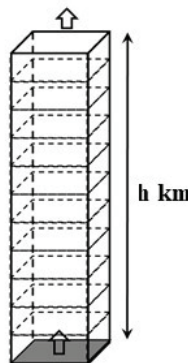
a) Horizontal Pipe Configuration



Pipe, length  $L$ , 1 to 7 km,

280 to 1000 ppm  $\text{CO}_2$  in dry air at 1 atm.

b) Vertical Atmospheric Path Configuration



Variable height,  $h$ , 1 to 11 km

300 or 600 ppm  $\text{CO}_2$  concentration

Dry air at 1 atm. or moist air 85%  
RH at surface

Vertical profile of temperature,  
pressure and humidity calculated for  
each 100 m layer.

Figure A1: Configurations used for the pipe and atmospheric absorption calculations.

Range $\text{cm}^{-1}$	Start/End	300 ppm	600 ppm
32	568 to 600 $\text{cm}^{-1}$	0.51	0.64
20	600 to 620 $\text{cm}^{-1}$	0.94	0.99
20	620 to 640 $\text{cm}^{-1}$	0.99	1.00
60	640 to 700 $\text{cm}^{-1}$	1.00	1.00
25	700 to 725 $\text{cm}^{-1}$	0.99	1.00
25	725 to 750 $\text{cm}^{-1}$	0.89	0.97
20	750 to 770 $\text{cm}^{-1}$	0.39	0.53
<b>Band Average</b>			
202	568 to 770 $\text{cm}^{-1}$	0.84	0.89
	<b>Absn coeff -ln(1-A)</b>	<b>1.83</b>	<b>2.21</b>
	<b>a (<math>\text{atm}^{-1} \text{m}^{-1}</math>)</b>	<b>0.870</b>	<b>0.527</b>

Table A1: The weighted averages of the seven spectral ranges are combined to give the band average absorption.

R. Clark, April 28<sup>th</sup> 2019

ppm	280	300	380	400	600	760	1000
1 km	0.62	0.63	0.66	0.66	0.71	0.73	0.76
2 km	0.70	0.71	0.73	0.74	0.78	0.81	0.83
3 km	0.75	0.75	0.78	0.78	0.82	0.84	0.87
5 km	0.80	0.81	0.83	0.83	0.87	0.88	0.90
7 km	0.83	0.84	0.86	0.86	0.89	0.90	0.92

Table A2: ‘Pipe’ absorption for selected path lengths from 1 to 7 km,  $CO_2$  concentrations of 280 to 1000 ppm, 568 to 769  $cm^{-1}$  spectral range, 293 K.

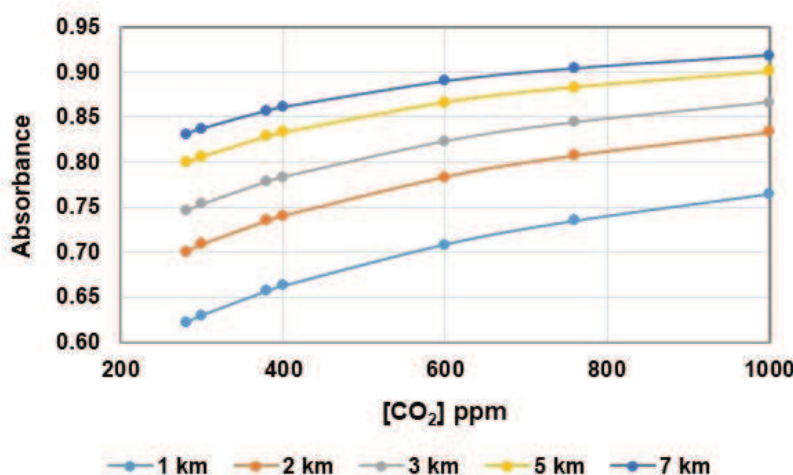


Figure A2: Data plotted from Table A2.

ppm	280	300	380	400	600	760	1000
1 km	0.78	0.79	0.82	0.83	0.87	0.89	0.92
2 km	0.86	0.87	0.89	0.90	0.93	0.95	0.97
3 km	0.90	0.91	0.93	0.93	0.96	0.97	0.98
5 km	0.94	0.95	0.96	0.97	0.98	0.99	0.99
7 km	0.96	0.97	0.98	0.98	0.99	1.00	1.00

Table A3: ‘Pipe’ Absorption for selected path lengths and concentrations, 1 to 7 km and 280 to 1000 ppm, 600 to 750  $cm^{-1}$  spectral range

The atmospheric radiative transfer calculations were performed using the same  $CO_2$  lines that were used for the ‘pipe’ calculations with  $^1H_2^{16}O$  lines with linestrengths  $> 1e-23$  added for the 85 % RH cases. The calculations were performed using Excel VBA macros at a spectral resolution of 0.01  $cm^{-1}$ . However, the data were binned into 1  $cm^{-1}$

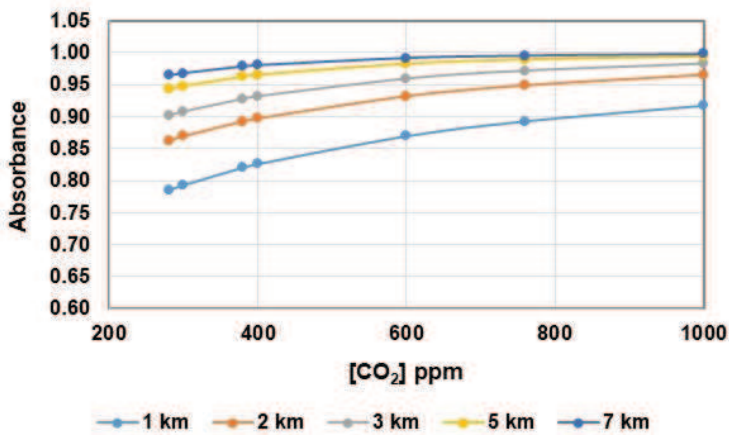


Figure A3: Data plotted from Table A3.

intervals for plotting. The conditions of temperature and  $CO_2$  concentration and the spectral ranges were the same as for the ‘pipe’ data. The  $H_2O$  concentration was set to a relative humidity of 85 % at 293 K for the first 100 m layer. The vertical path length was varied from 1 to 11 km in 1 km steps. The results are given in Tables A4 and A5. Plots of the data are shown in Figures A4 and A5.

Altitude km	568 to 769 cm <sup>-1</sup>	568 to 769 cm <sup>-1</sup>	600 to 750 cm <sup>-1</sup>	600 to 750 cm <sup>-1</sup>
	300 ppm	600 ppm	300 ppm	600 ppm
1	0.618	0.696	0.777	0.856
2	0.682	0.758	0.842	0.910
3	0.713	0.786	0.872	0.933
4	0.731	0.802	0.888	0.945
5	0.742	0.811	0.897	0.952
6	0.749	0.817	0.904	0.956
7	0.754	0.821	0.908	0.958
8	0.757	0.823	0.910	0.960
9	0.759	0.825	0.912	0.961
10	0.761	0.826	0.913	0.962
11	0.761	0.827	0.914	0.962

Table A4: Atmospheric absorption data for the spectral range from 568 to 769 cm<sup>-1</sup> and from 600 to 750 cm<sup>-1</sup>. The vertical heights from the surface were varied from 1 to 11 km.

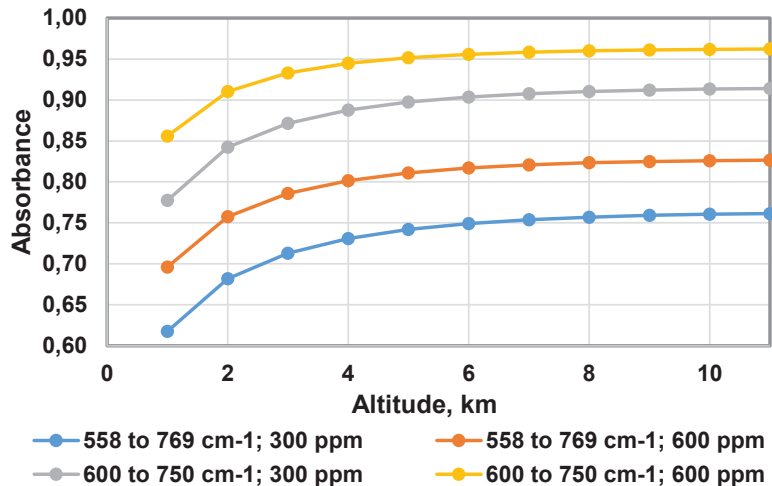


Figure A4: Data plotted from Table A4.

	558 to 769 cm <sup>-1</sup>	558 to 769 cm <sup>-1</sup>	600 to 750 cm <sup>-1</sup>	600 to 750 cm <sup>-1</sup>
Altitude km	300 ppm, 85 RH	600 ppm, 85 RH	300 ppm, 85 RH	600 ppm, 85 RH
1	0.799	0.843	0.856	0.904
2	0.854	0.892	0.906	0.945
3	0.876	0.910	0.927	0.961
4	0.887	0.919	0.937	0.968
5	0.894	0.924	0.943	0.973
6	0.897	0.927	0.947	0.975
7	0.900	0.929	0.949	0.977
8	0.901	0.930	0.951	0.977
9	0.902	0.931	0.952	0.978
10	0.903	0.931	0.952	0.978
11	0.903	0.929	0.953	0.977

Table A5: Atmospheric absorption data for the spectral range from 558 to 769 cm<sup>-1</sup> and from 600 to 750 cm<sup>-1</sup>. The vertical heights from the surface were varied from 1 to 11 km.

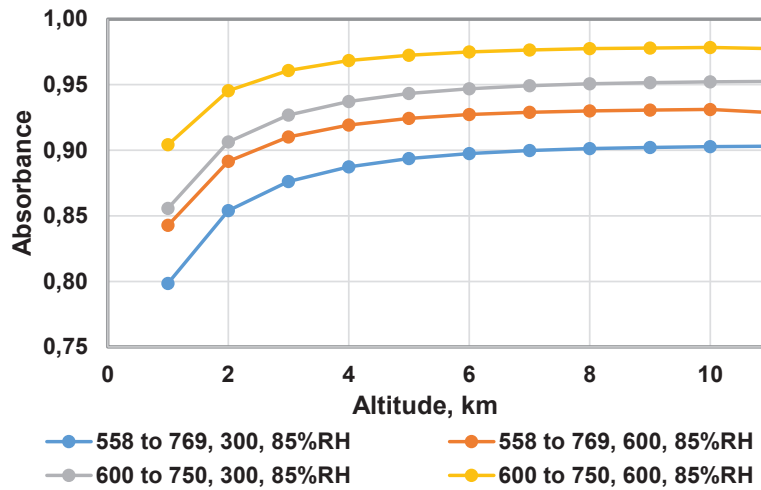


Figure A5: Data plotted from Table A5.

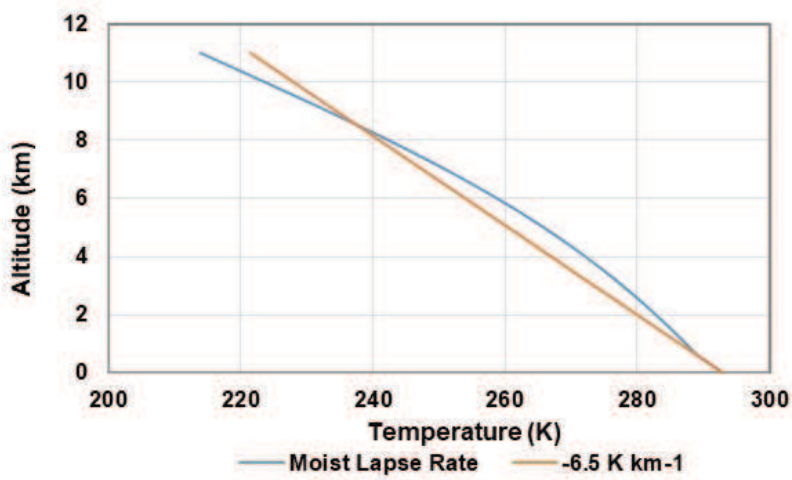


Figure A6: The lapse rates used in the atmospheric absorption calculations, from [14].

## B A Concise Representation of the Radiative “Greenhouse Effect” in the Atmosphere.

The surface of the earth receives a net radiation from the sun,  $S_0$ , of approximately  $S_0 \simeq 240 \text{ W m}^{-2}$ , see footnote 2 in the main text. The infrared radiation from the surface of the earth, the LWIR, contains a component,  $S_W$ , restricted in its spectral range to the so-called “atmospheric window”, and a second component,  $S_{up}$ . The second component consists of a small part,  $f' S_{up}$  ( $f' \ll 1$ ), emitted to space, and a larger fraction,  $(1-f') S_{up}$  that is absorbed by the so-called “greenhouse gases”, essentially  $H_2O$  and  $CO_2$ , in the atmosphere, and subsequently re-emitted, partly to space,  $A_{up}$ , and partly down to the surface,  $A_{down}$ , compare fig. B1.

The “transmittance parameter”  $f'$ , with  $0 \leq f' \leq 1$ , realistic values being restricted to  $f' \ll 1$ , quantifies the transmittance of the earth’s surface radiation in the spectral range outside the atmospheric window. Compare the incomplete saturation of the absorption in fig. 4a at altitudes larger than (approximately) 9 km.

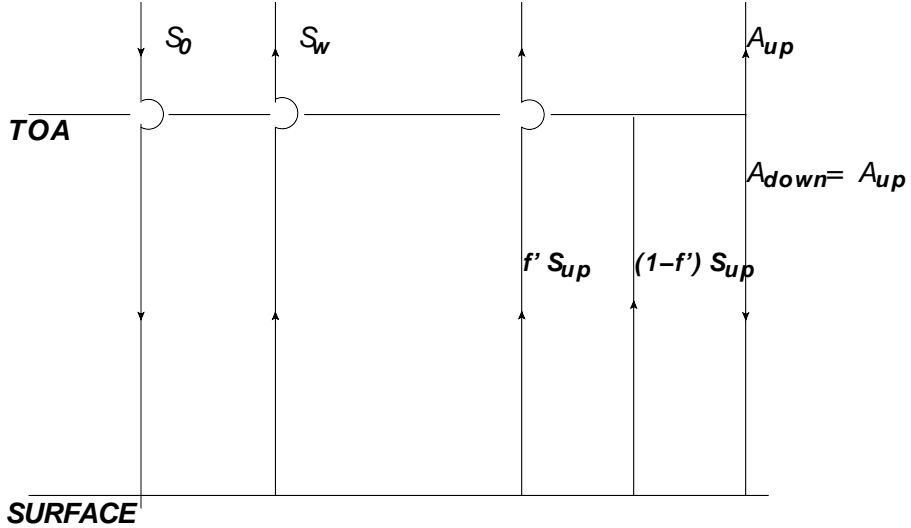


Figure B1: Schematic representation of the net radiation from the sun,  $S_0 \simeq 240 \text{ W m}^{-2}$ , the infrared radiation to space through the atmospheric window,  $S_W$ , the infrared radiation from the surface to space  $f' S_{up}$ , and to the atmosphere  $(1-f') S_{up}$ , where  $f' \ll 1$ , and the radiation from the atmosphere to space  $A_{up}$  and to the surface,  $A_{down}$ .

Global radiative equilibrium of the earth is due to an equality between the intensity of the short-wave radiation received from the sun,  $S_0$ , and the infrared radiation sent out to space, i.e.

$$S_0 = S_W + f' S_{up} + A_{up}. \quad (\text{B.1})$$

Equilibrium at the upper atmosphere (the top of the atmosphere, TOA) requires

$$(1 - f')S_{up} = A_{up} + A_{down} = 2A_{up}, \quad (\text{B.2})$$

where equality of the upward and the downward emission from the greenhouse gases has been employed in the second step. From (B.1) and (B.2), we deduce the radiation from the surface,  $S_{up}$ , given by

$$S_{up} = \frac{2}{1 + f'}(S_0 - S_W), \quad (\text{B.3})$$

as well as the radiation from the TOA,

$$A_{up} = A_{down} = \frac{1 - f'}{1 + f'}(S_0 - S_W). \quad (\text{B.4})$$

Both,  $S_{up}$  and  $A_{up}$  are expressed in terms of  $S_0 - S_W$ , that is the radiation from the sun upon reduction by the radiation,  $S_W$ , that is associated with the transmission of radiation through the atmospheric window.

For given  $S_0$ , from (B.3), we find that the total emission by the surface,  $S_{tot,surf}(S_W, f')$ , is given by

$$S_{tot,surf}(S_W, f') = S_W + S_{up} = S_0 \left( \frac{2}{1 + f'} - \frac{S_W}{S_0} \frac{1 - f'}{1 + f'} \right) \equiv S_0 c \left( \frac{S_W}{S_0}, f' \right). \quad (\text{B.5})$$

Employing (B.3) and (B.4), one may explicitly check the validity of equilibrium at the surface,

$$S_{tot,surf} = S_W + S_{up} = S_0 + A_{down} = S_0 + A_{up}. \quad (\text{B.6})$$

The radiation to space at the TOA,

$$S_{tot,TOA}(S_W, f') = S_W + f' S_{up} + A_{up}, \quad (\text{B.7})$$

upon substitution of the results for  $S_{up}$  and for  $A_{up}$  from (B.3) and (B.4) becomes

$$S_{tot,TOA}(S_W, f') = S_0. \quad (\text{B.8})$$

Global radiative equilibrium (B.1) is realized by the equality of the radiation intensities emitted from the TOA,  $S_{tot,TOA}$ , and received from the sun,  $S_0$ .

It will be illuminating to numerically evaluate our main result, the expression for the surface radiation (B.5), for several relevant values of  $S_W$  and  $f'$  for fixed  $S_0 = 240 \text{ W m}^{-2}$ .

Upon assuming a Planck black-body radiation spectrum for the surface radiation (B.5),

$$S_{tot,surf}(S_W, f') = \sigma (T_{surf}(S_W, f'))^4, \quad (\text{B.9})$$

where  $\sigma \cong 5.670 \times 10^{-8} \text{ W m}^{-2} \text{ K}^{-4}$ , we obtain the associated surface temperature,

$$\begin{aligned} T_{surf}(S_W, f') &= \left( \frac{S_0}{\sigma} \right)^{\frac{1}{4}} \left( \frac{2}{1 + f'} - \frac{S_W}{S_0} \frac{1 - f'}{1 + f'} \right)^{\frac{1}{4}} \\ &= 255.069 \left( \frac{2}{1 + f'} - \frac{S_W}{S_0} \frac{1 - f'}{1 + f'} \right)^{\frac{1}{4}} K \\ &= 255.069 c \left( \frac{S_W}{S_0}, f' \right)^{\frac{1}{4}} K. \end{aligned} \quad (\text{B.10})$$

Relations (B.5) and (B.10) give the equilibrium surface radiation and surface temperature for given values of  $S_0$ ,  $S_W$  and  $f'$ .

The numerical results for  $S_{tot,surf}$  from (B.5) and  $T_{surf}$  from (B.10) for a few representative values of  $S_W$  are collected in Table B1.

$S_W[Wm^{-2}](f')$	$c\left(\frac{S_W}{S_0}, f'\right)$	$S_{tot,surf}[Wm^{-2}]$	$T_{surf}[K]$
240 and/or $f' = 1$	1.0	240	$255 = -18^0 \text{ C}$
58 ( $f' = 0.1$ )	1.62	389	$288 = 15^0 \text{ C}$
43 ( $f' = 0.1$ )	1.67	401	$290 = 17^0 \text{ C}$
28 ( $f' = 0.1$ )	1.72	413	$292 = 19^0 \text{ C}$
0 ( $f' = 0.1$ )	1.82	436	$296 = 23^0 \text{ C}$
0 ( $f' = 0$ )	2.0	480	$303 = 30^0 \text{ C}$

Table B1: Numerical results for the total surface radiation  $S_{tot,surf}(S_W, f')$  given by (B.5), and for the surface temperature  $T_{surf}(S_W, f')$  given by (B.10).

Turning to a discussion of the results in Table B1, we start with the results for the empirical input of  $S_W = 43 \pm 15Wm^{-2}$ , or  $58 \geq S_W \geq 28Wm^{-2}$ , deduced [15] from meteorological measurements of the long-wave infrared radiation (LWIR). The value of  $f' = 0.1$  follows from Table 4a in the main text. At the saturation limit (for  $CO_2$  content of 300 ppm) the absorption reaches a value of  $A = 0.90$ . This corresponds to  $(1 - f')S_{up} = 0.90S_{up}$ , or  $f' = 0.1$ . The results for the surface temperature,  $T_{surf}$ , from (B.10) given by  $288 \leq T_{surf} \leq 292K$ , or  $15^0 \text{ C}$  to  $19^0 \text{ C}$ , are consistent with the very elaborate theoretical analysis in refs. [4] and [10].

The case of  $S_W = S_0 = 240Wm^{-2}$  in the first line of Table B1, according to (B.3) and (B.4), corresponds to  $S_{up} = A_{up} = 0$ . This is the hypothetical case of an atmosphere allowing for direct total emission from the surface to space, or zero absorption, no greenhouse gas present. Comparing  $S_{tot,surf}(S_W = S_0, f')$  with (B.8), we find the identity

$$S_{tot,TOA}(S_W, f') = S_{tot,surf}(S_W = S_0, f'). \quad (\text{B.11})$$

The infrared radiation at the TOA,  $S_{tot,TOA}(S_W, f') = S_0$ , is equal to the surface radiation of a non-absorbing hypothetical atmosphere<sup>8</sup>. The associated temperature is given by  $T_{TOA} = T_{surf} = 255K$ . The “greenhouse effect” of the atmosphere containing “greenhouse

<sup>8</sup>Equivalently, the non-absorbing atmosphere may be described by inserting  $f' = 1$  in (B.5), implying  $S_{tot,surf}(S_W, f' = 1) = S_0$  and  $A_{up} = A_{down} = 0$  according to (B.4).

gases” consists of shifting the origin of the outgoing infrared radiation (responsible for equilibrium with the radiation from the sun) from the surface to the TOA.

The hypothetical limit of  $S_W = 0$  and  $f' = 0$  in the last line of Table B1 describes the case of a hypothetical “closed atmospheric window”, total absorption of the emitted surface radiation of  $S_{tot, surf}(S_W = 0, f' = 0) = 2S_0$ , implying the maximally possible equilibrium surface temperature of  $T_{surf} = 303K = 30^0C$ .

A comment on the consistency of our results with the radiation and energy budget analysis in ref. [4] is appropriate. Trenberth et al. [4], using  $S'_0 = 239Wm^{-2}$  as input solar radiation, find a total surface radiation,  $S'_{tot, surf} = 396Wm^{-2}$  corresponding to  $T' = 289K = 16^0C$ , consistent with our result from Table B1,  $S_{tot, surf} \simeq 401Wm^{-2}$  and  $T = 17^0C$ . The consistency is not accidental, but can be understood as follows.

According to ref. [4], in our notation, the downward radiation is given by  $A'_{down} = 333Wm^{-2}$ . Including the amount of  $78Wm^{-2}$  [4] of solar radiation absorbed by the atmosphere into the solar radiation absorbed by the surface, one effectively has  $A''_{down} = 333 - 78 = 255Wm^{-2}$ . Thermals and evaporation amount to  $97Wm^{-2}$  [4]. From our point of view they should be considered as being independent from the radiation budget. The amount of  $97 Wm^{-2}$  quantifies the energy conversion of an adiabatic heat engine working between the temperatures of  $T = 289K$  on the surface, and  $T = 255K$  at the TOA. The heat engine, working in the gravitational field of the earth, solely continuously converts internal energy of the air at  $T = 289K$  back and forth into potential energy at  $T = 255K$ . This process does not affect the radiative balance, and accordingly,  $A'_{down} = 333Wm^{-2}$  is reduced to  $A'''_{down} = 333 - 78 - 97 = 158Wm^{-2}$ , a value consistent with  $A_{down} = 161Wm^{-2}$  from (B.4).

The radiation balance obtained by Trenberth et al. [4] accordingly is consistently reduced to the simple representation shown in fig. C1 that contains the essential features of the greenhouse effect.

We turn to the change of the surface radiation under doubling of the atmospheric  $CO_2$  content, and the associated change of the surface temperature  $\Delta T$  discussed in section 3 of the main text.

For a small change of the parameter  $f' \rightarrow f' + \Delta f'$ , with  $S_W = const$ , from (B.5) and (B.6) we find

$$\frac{dS_{up}(S_W, f')}{df'} = \frac{dS_{tot, surf}(S_W, f')}{df'} = -\frac{2(S_0 - S_W)}{(1 + f')^2}, \quad (B.12)$$

or

$$\Delta f' = -\frac{(1 + f')^2}{2(S_0 - S_W)} \Delta S_{up} = -\frac{(1 + f')^2}{2(S_0 - S_W)} \Delta_{2\times CO_2}, \quad (B.13)$$

where  $\Delta S_{up} = \Delta S_{tot, surf} = \Delta_{2\times CO_2}$ , due to  $CO_2$  doubling, was inserted in the second step. The negative value of  $\Delta f' < 0$  for  $\Delta_{2\times CO_2} > 0$  implies less direct radiation to space and, accordingly, a rise of the surface temperature,  $\Delta T > 0$ .

For the change of the surface temperature  $T_{surf}$ , from (B.10), we obtain

$$\Delta T = \frac{dT}{df'} df' = -\frac{T_{surf}}{4} \frac{2 \left(1 - \frac{S_W}{S_0}\right)}{2(1 + f') - \frac{S_W}{S_0}(1 - f'^2)} \Delta f' = \frac{T_{surf}}{4} \frac{\Delta_{2\times CO_2}}{S_{tot, surf}(S_W, f')}, \quad (B.14)$$

where  $\Delta f'$  from (B.13) was inserted in the last step. The expression resulting from the insertion was simplified to yield the expression for  $S_{tot, surf}(S_W, f')$  in (B.5) in the denominator of (B.14).

The agreement of  $\Delta T$  in (B.14) with  $\Delta T$  in (3.3) of the main text comes without surprise. We note however, that the present derivation of (B.14), relying on (B.5) and (B.10), assures equilibrium of radiation at the earth's surface and at the TOA for any given values of  $S_0, S_W, f'$ , and for  $f' \rightarrow f' + \Delta f'$  in particular. In slight distinction from the present derivation of (B.14), in (3.3), we relied on using restoration of equilibrium upon  $CO_2$  doubling. It is noteworthy, moreover, that  $T_{surf}$  in (B.10) and  $\Delta T$  in (B.14) is predicted from the empirically known values of  $S_0, S_W$  and  $f'$ , while  $T_{surf}$  in (3.3) was used as an input parameter.

$S_W[Wm^{-2}](f')$	$c\left(\frac{S_W}{S_0}, f'\right)$	$S_{tot, surf}[Wm^{-2}]$	$T_{surf}[K]$
43 ( $f' = 0.100$ )	1.67159	401.182	290.028
43 ( $f' = 0.092015$ )	1.68250	403.800	290.500
		$\Delta S_{up} = \Delta_{2\times CO_2} = 2.6$	$\Delta T = 0.47$

Table B2: Numerical results for the total surface radiation  $S_{tot, surf}(S_W, f')$  according to (B.5), and the surface temperature, given by (B.10), as well as the temperature difference consistently also obtained from (B.14).

The numerical results in Table B2 are based on the input parameters,  $S_0 = 240 Wm^{-2}$  and  $S_W = 43 Wm^{-2}$ , as well as  $f' = 0.1$  and  $f' = 0.1 + \Delta f' = 0.092015$ , as obtained by evaluation of (B.13) for  $\Delta_{2\times CO_2} = 2.6 Wm^{-2}$  taken from Table 4a.

In a first step, upon evaluating (B.5) and (B.10), we obtained the surface radiation and surface temperature shown in the second and third lines of Table B2. The subtraction of the two surface temperatures from each other then yields  $\Delta T = 0.47 K$  shown in the last line of Table B2. In a second step, we confirm  $\Delta T = 0.47 K$ <sup>9</sup> by evaluating (B.14) by either inserting  $\Delta f'$  from (B.13) or by directly inserting  $\Delta_{2\times CO_2} = 2.6 Wm^{-2}$ .

---

<sup>9</sup>The discrepancy between  $\Delta T = 0.47 K$  in Table B2 and  $\Delta T = 0.46 K$  in Table 5 of the main text is due to the different input of  $T = 293 K$  in the main text.